

Meson cloud and $SU(3)$ symmetry breaking in parton distributions

F. Carvalho^a, F.O. Durães^b, F.S. Navarra^c, M. Nielsen^d, F.M. Steffens^e

Instituto de Física, Universidade de São Paulo, C.P. 66318, 05315-970 São Paulo, SP, Brazil

Received: 28 July 2000 / Published online: 23 October 2000 – © Springer-Verlag 2000

Abstract. We apply the meson cloud model to the calculation of non-singlet parton distributions in the nucleon sea, including the octet and the decuplet cloud baryon contributions. We give special attention to the differences between non-strange and strange sea quarks, trying to identify possible sources of $SU(3)$ flavor breaking. An analysis in terms of the κ parameter is presented, and we find that the existing $SU(3)$ flavor asymmetry in the nucleon sea can be quantitatively explained by the meson cloud. We also consider the Σ^+ baryon, finding similar conclusions.

1 Introduction

The presence of a flavor asymmetry in the light antiquark sea of the proton is now clearly established [1, 2]. It can be expressed either in terms of the difference $\Delta(x) = \bar{d}(x) - \bar{u}(x)$, or in terms of the ratio $R(x) = \bar{d}(x)/\bar{u}(x)$. The fact that this difference is larger than zero (or that the ratio is larger than one) is usually referred to as $SU(2)$ flavor symmetry breaking in the proton sea.

We will discuss in this paper the non-perturbative origin of the breaking of flavor symmetry, both at the $SU(2)$ and at the $SU(3)$ level. To this end, we will study the suppression factor of \bar{u} antiquarks in the $SU(2)$ case, defined as

$$\kappa_{(2)} = \frac{\int_0^1 dx x \bar{d}(x, \mu^2)}{\int_0^1 dx x \bar{u}(x, \mu^2)}, \quad (1)$$

and the suppression factor of strangeness in the $SU(3)$ case:

$$\kappa_{(3)} = \frac{\int_0^1 dx [xs(x, \mu^2) + x\bar{s}(x, \mu^2)]}{\int_0^1 dx [x\bar{u}(x, \mu^2) + x\bar{d}(x, \mu^2)]}. \quad (2)$$

We notice that in the limit of exact $SU(2)$ ($SU(3)$) flavor symmetry $\kappa_{(2)} = 1$ ($\kappa_{(3)} = 1$). The CCFR collaboration has measured [3] $\kappa_{(3)} \simeq 0.37 \pm 0.05$ (0.477 ± 0.05) in an LO (NLO) QCD analysis. Uncertainties apart, it is clear that there is a substantial violation of the $SU(3)$ flavor symmetry. In the non-strange light antiquark sector, the use of the standard parameterizations leads to $\kappa_{(2)} \sim 1.3$ [4, 5], indicating also a strong violation of the $SU(2)$ flavor

symmetry in the proton sea. At the same time, the $SU(2)$ charge symmetry is believed to hold within the baryon octet, i.e., $\bar{d}(x) - \bar{u}(x)$ in the proton is equal to $\bar{u}(x) - \bar{d}(x)$ in the neutron. An interesting question is how $SU(3)$ charge symmetry is broken within the baryon octet. If the symmetry were exact, this would mean, for instance, that $s(x) - \bar{s}(x)$ in the proton should be equal to $d(x) - \bar{d}(x)$ in the Σ^+ . However, as calculated by the authors of [7–9], this is not the case, and in the present work we also investigate the origins of the breaking of this symmetry.

In QCD, exact $SU(3)$ symmetry implies that the u , d and s quarks have the same mass. Since the strange quark mass, m_s , is significantly larger than the up and down quark masses, the symmetry is only approximate. At the hadronic level, exact $SU(3)$ symmetry also implies that the masses of baryons or mesons belonging to the same multiplets are all equal. Clearly this is not the case and the masses within the baryon multiplets differ among themselves by more than 30%. The mass discrepancy is even more pronounced in the meson octet.

Another consequence of the $SU(3)$ symmetry at the hadronic level is that the coupling constant in a generic baryon–baryon–meson ($g\bar{B}\gamma_5 BM$) vertex should be the same for all of B , \bar{B} and M . Since these three states together must form a $SU(3)$ singlet state, and the mesons are usually in octet states, it follows that the product of the two baryon representations must also be in a $SU(3)$ octet state. Out of the $(\bar{B}B)$ product 8×8 , we get two distinct octets and therefore two independent coupling constants. This is the origin of the two $SU(3)$ constants, F and D . When we consider some particular baryon–baryon–meson vertices, additional (Clebsch–Gordan) factors appear, so that the final couplings are different from each other. However, exact $SU(3)$ symmetry imposes well-defined connections between them. Finally, the analysis of

^a e-mail: babi@if.usp.br

^b e-mail: fduraes@if.usp.br

^c e-mail: navarra@if.usp.br

^d e-mail: mnielsen@if.usp.br

^e e-mail: fsteffen@if.usp.br

the experimental data determines the relation between F and D in terms of the parameter [10]

$$\alpha_D = \frac{D}{D+F} \simeq 0.64. \quad (3)$$

We can make use of QCD sum rules (QCDSR) to calculate the above mentioned coupling constants [11,12]. In this approach we are able to identify the $SU(3)$ breaking sources affecting the couplings, which are mainly the quark and hadron mass differences. The different values of the condensates and other QCDSR parameters also play an important role.

As for the origin of the asymmetry in the light anti-quark distributions, there are now strong indications that part of the nucleon sea comes from fluctuations of the original nucleon into baryon–meson states, i.e., from the meson cloud [13–16]. The meson cloud model (MCM) is dominated by hadronic quantities like hadron masses and coupling constants. This bridge between the physics of parton distributions and the conventional hadron physics may also help us, by connecting one with the other, to understand both $SU(3)$ symmetry breaking at the hadron and parton levels.

2 Parton distributions in the MCM

In what follows, we show the meson–baryon Fock decomposition of the proton and of the Σ^+ . In the case of the proton, most of the material has already been presented elsewhere [14–16]. We include it here just for completeness. Parton distributions in the Σ^+ hyperon have been discussed in [7–9], and we will also address them in this work. This will enable us to make a close comparison between the proton and hyperon parton distributions.

2.1 The proton

As usual, we decompose the proton in the following possible Fock states:

$$\begin{aligned} |p\rangle = & Z[|p_0\rangle + |p_0\pi^0\rangle + |n\pi^+\rangle + |\Delta^0\pi^+\rangle + |\Delta^+\pi^0\rangle \\ & + |\Delta^{++}\pi^-\rangle + |\Lambda K^+\rangle + |\Sigma^0 K^+\rangle + |\Sigma^{0*} K^+\rangle \\ & + |\Sigma^+ K^0\rangle + |\Sigma^{+*} K^0\rangle], \end{aligned} \quad (4)$$

where $|p_0\rangle$ is the bare proton. We consider only light mesons. The relative normalization of these states is, in principle, fixed once the cloud parameters are given. The normalization constant Z measures the probability to find the proton in its bare state.

In the $|MB\rangle$ state, the meson and the baryon have fractional momentum y_M and y_B , with distributions $f_{M/MB}(y_M)$ and $f_{B/MB}(y_B)$, respectively. Of course $y_M + y_B = 1$ and these distributions are related by

$$f_{M/MB}(z) = f_{B/MB}(1-z). \quad (5)$$

The splitting function $f_{M/MB}(y)$ represents the probability density to find a meson with momentum fraction y of the nucleon and is usually given by [14]

$$\begin{aligned} f_{M/MB}(y) &= \frac{g_{MBp}^2}{16\pi^2} y \int_{-\infty}^{t_{\max}} dt \frac{[-t + (M_B - M_p)^2]}{[t - m_M^2]^2} F_{MBp}^2(t), \end{aligned} \quad (6)$$

for baryons (B) belonging to the octet, and

$$\begin{aligned} f_{M/MB}(y) &= \frac{g_{MBp}^2}{16\pi^2} y \int_{-\infty}^{t_{\max}} dt \\ &\times \frac{[(M_B + M_p)^2 - t]^2 [(M_p - M_B)^2 - t]}{12M_B^2 M_p^2 [t - m_M^2]^2} F_{MBp}^2(t), \end{aligned} \quad (7)$$

for baryons belonging to the decuplet. In the calculations we need the baryon–meson–baryon form factors appearing in the splitting functions. Following a phenomenological approach, we use the dipole form:

$$F_{MBp}(t) = \left(\frac{\Lambda_{MBp}^2 - m_M^2}{\Lambda_{MBp}^2 - t} \right)^2, \quad (8)$$

where Λ_{MBp} is the form factor cut-off parameter. In the above equations t and m_M are the four-momentum square and the mass of the meson in the cloud state, and t_{\max} is the maximum t given by

$$t_{\max} = M_p^2 y - \frac{M_B^2 y}{1-y}, \quad (9)$$

where M_B (M_p) is the mass of the baryon (proton). Since the function $f_{M/MB}(y)$ has the interpretation of a flux of mesons inside the proton, the corresponding integral,

$$n_{M/MB} = \sum_{MB} \int_0^1 dy f_{M/MB}(y), \quad (10)$$

can be interpreted as the number of mesons in the proton, or the number of mesons in the air. In many works, the magnitude of the multiplicities $n_{M/MB}$ has been considered as a measure of the validity of MCM in the standard formulation with MB states. If these multiplicities turn out to be large ($\simeq 1$) then there is no justification for employing a one-meson truncation of the Fock expansion, as the expansion ceases to converge. This may happen for large cut-off values.

Once the splitting functions (6) and (7) are known we can calculate the antiquark distribution in the proton coming from the meson cloud through the convolution

$$\bar{q}_f(x) = \sum_{MB} \int_x^1 \frac{dy}{y} f_{M/MB}(y) \bar{q}_f^M\left(\frac{x}{y}\right), \quad (11)$$

where $\bar{q}_f^M(z)$ is the valence antiquark distribution of flavor f in the meson. An analogous expression holds for the quark distributions. In performing the calculations we will need parameterizations for the valence quark distributions in the pions and kaons. These are taken from the literature and are given in the appendix. We are not including the effects of sea quarks in the mesons.

With the above formula we can compute the \bar{d} and \bar{u} distributions, their difference, $\bar{d}(x) - \bar{u}(x)$, and hence the Gottfried integral:

$$S_G = \frac{1}{3} - \frac{2}{3} \int_0^1 [\bar{d}(x) - \bar{u}(x)] dx. \quad (12)$$

Before making a quantitative analysis of the $\bar{d}(x) - \bar{u}(x)$ difference we note that, apart from the meson cloud, there could be some other non-perturbative physics necessary to understand the experimental results. In particular, it is natural to include the effects from the Fermi statistics of the quarks, as suggested long ago by Field and Feynman [22], and implemented recently in a quantitative way [15]. The idea is quite straightforward: as the proton is, primarily, a uud state, it should be easier to insert a $d\bar{d}$ pair than a $u\bar{u}$ pair in the proton sea. This follows from the fact that there are more empty states for the insertion of a d quark than for the insertion of a u quark¹. Following [15], we parameterize this Pauli-blocking (PB) contribution by

$$(\bar{d} - \bar{u})^{\text{PB}}(x) = \Delta^{\text{PB}}(n+1)(1-x)^n. \quad (13)$$

As part of the non-perturbative sea, the PB contribution is added to the $\bar{d}(x) - \bar{u}(x)$ difference coming from the meson cloud, computed from (11).

In our quantitative analysis we have first to fix the inputs for the calculations (couplings and masses), then adjust the parameters (two form factor cut-off parameters, Δ^{PB} and the power n of (13)) by fitting the experimental data and after that make predictions, especially for strange partons distributions.

The coupling constants are chosen to be compatible with $SU(3)$ symmetry, i.e., they all follow $SU(3)$ relations [17]. Of course, the non-strange subset of these couplings respects the $SU(2)$ (isospin) symmetry. The cut-off parameters are also chosen to be compatible with $SU(3)$ symmetry, i.e., they are all equal within $SU(3)$ multiplets. As will be seen below, these choices not only reduce the number of free parameters but will also allow us to recover the $SU(3)$ limit.

The masses are $m_p = m_n = 938$ MeV, $m_\pi = 138$ MeV, $m_K = 480$ MeV, $m_\Delta = 1232$ MeV, $m_\Lambda = 1116$ MeV, and $m_\Sigma = 1189$ MeV. The octet coupling constants are given by the expressions in Table 1 [17], where $g_{p\pi^0 p} = -13.45$ [18,19] and α_D was given in (3). For the decuplet coupling constants, in Table 2, where $g_{p\Delta^0 \pi^+} = 28.6/6^{1/2}$ [20, 21], we also use the standard $SU(3)$ relations between the couplings [17].

The four parameters are adjusted by simultaneously fitting the E866 data on $\bar{d}(x) - \bar{u}(x)$ and $\bar{d}(x)/\bar{u}(x)$ and the leading pion and kaon spectra measured in [25,26]. A similar fitting procedure has already been adopted by many authors working in the meson cloud approach. What is new in our work is that we use a larger amount of experimental sources.

¹ As shown in [23,24], possible antisymmetrization effects between the sea and the valence quarks can spoil this naive counting

Table 1. Octet coupling constants

$g_{pK^+\Lambda}$	$-1/(3^{1/2})(3 - 2\alpha_D)g_{p\pi^0 p}$
$g_{pK^+\Sigma^0}$	$(2\alpha_D - 1)g_{p\pi^0 p}$
$g_{pK^0\Sigma^+}$	$2^{1/2}(2\alpha_D - 1)g_{p\pi^0 p}$
$g_{p\pi^+n}$	$2^{1/2}g_{p\pi^0 p}$

Table 2. Decuplet coupling constants

$g_{p\Sigma^{0*}K^+}$	$(2^{1/2})/(2)g_{p\Delta^0 \pi^+}$
$g_{p\Sigma^{*+}K^0}$	$g_{p\Delta^0 \pi^+}$
$g_{p\Delta^+\pi^0}$	$2^{1/2}g_{p\Delta^0 \pi^+}$
$g_{p\Delta^{++}\pi^-}$	$3^{1/2}g_{p\Delta^0 \pi^+}$

All the analyses performed so far indicate that, given the theoretical uncertainties, it is meaningless to search for very accurate values of these cut-off parameters. It is presently not possible to reduce their uncertainties down to less than 100 MeV. Therefore we will not try here to carry out a least χ^2 analysis. Many of the works [14–16] done on this subject indicate that the cut-off parameters must be soft ($\Lambda \simeq 1$ GeV in dipole form). Indeed, in our attempt to have a simultaneous description of the difference $\Delta(x)$, the ratio $R(x)$ (as defined below) and the x_F spectra of pions and kaons we find that

$$\Lambda_{\text{oct}} = 1.10 \text{ GeV} ; \Lambda_{\text{dec}} = 1.07 \text{ GeV}; \\ \Delta^{\text{PB}} = 0.017; n = 10, \quad (14)$$

where Λ_{oct} and Λ_{dec} are the cut-off parameters for all the octet and decuplet vertices, respectively. We notice that the ratio and the difference are related by [1]

$$R(x) = \frac{1 + \Delta(x)/\Sigma(x)}{1 - \Delta(x)/\Sigma(x)}, \quad (15)$$

where $\Sigma(x) = \bar{d}(x) + \bar{u}(x)$ is the total antiquark distribution, which may be taken from any of the available parameterizations of the parton distributions and $\Delta(x) = \bar{d}(x) - \bar{u}(x)$. We follow the E866 collaboration² and use the CTEQ parameterization for $\Sigma(x)$ and the MCM calculation for $\Delta(x)$.

We point out that it is crucial for our later discussion of $SU(3)$ symmetry breaking that the cut-off parameters be the same for all the members of the multiplets, including the cut-offs involved in the production of strangeness. Their exact values could be different, provided that all the constraints imposed by convergence of the Fock expansion, by data on inclusive meson production or any other experimental information, be satisfied. In any case, we stress that the cut-offs were fixed in the reproduction of the mentioned experimental data, and the results presented here,

² As the E866 collaboration measured $R(x)$ and used the CTEQ [6] parameterization for $\Sigma(x)$ to determine $\Delta(x)$, we are just following the inverse path. This is the most consistent way, according to what was done in [1], to obtain $R(x)$ from $\Delta(x)$

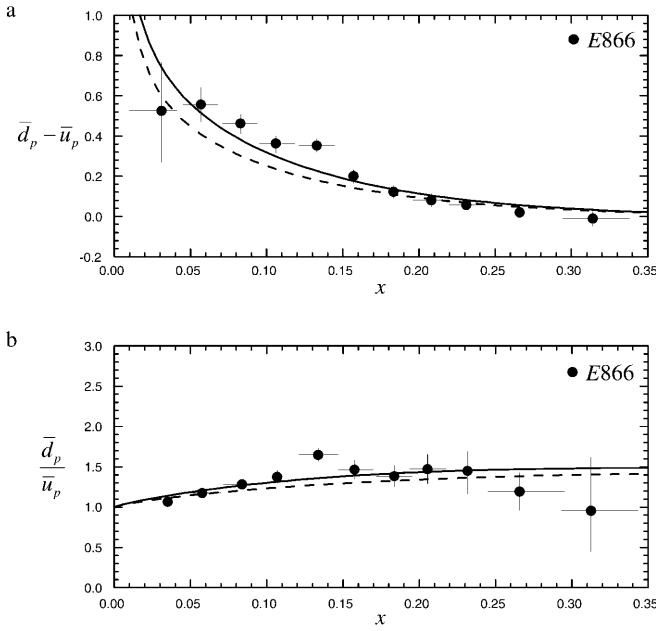


Fig. 1. **a** $\bar{d}(x) - \bar{u}(x)$ calculated with (11) compared with E866 data; **b** same as **a** for the ratio $\bar{d}(x)/\bar{u}(x)$. The dashed lines represent our result without Pauli blocking

which include the strange sector, are predictions of the model.

The solid lines in Figs. 1a,b show the combined effect of meson cloud and PB effects for the $\bar{d}(x) - \bar{u}(x)$ and for $\bar{d}(x)/\bar{u}(x)$, as a function of x . The dashed lines show the effect of the meson cloud alone. The data points are from the E866 collaboration [1, 2], where the CTEQ [6] parameterization for $\bar{u}(x) + \bar{d}(x)$ was used in (15) to relate $\Delta(x)$ to $R(x)$. Our results confirm analogous calculations performed previously by Melnitchouk, Speth and Thomas [15], although we see that the size of our PB is significantly smaller. This difference appears because we use more states in our Fock decomposition of the proton and consequently find different values for the cut-off parameters. We also use a slightly different parameterization of the form factors.

In Figs. 2a,b we show respectively our fits of the pion and kaon spectra measured in [25, 26] using the parameters (14). The formulas used in computing the spectra are given in detail in [16]. The expressions are exactly the same, only the parameters are different³. In [16] we had already found a set of cut-off parameter values lying around 1 GeV. The present calculation is an improvement over the previous one because we are now including the perturbative effects in the ratio $\bar{d}(x)/\bar{u}(x)$ and also including Pauli-blocking effects.

When working with the sea parton distributions it should be emphasized that in differences such as $\bar{d}(x) - \bar{u}(x)$ or $\bar{s}(x) - \bar{u}(x)$ the perturbative contributions should cancel if the production of sea partons from hard gluons is to be insensitive to small masses, including the strange

³ The cut-offs are as in (14) and $K_{abs} = 0.2$ both for pions and kaons

quark mass. Such a property was already used in the writing of (15). Therefore, any deviation of $\kappa_{(2)}$ and $\kappa_{(3)}$ from 1 (or $x(\bar{d}(x) - \bar{u}(x))$, etc., from zero), must have a non-perturbative origin. As the meson cloud is the main non-perturbative contribution, it should be quite reliable when calculating the differences of sea distributions. Figure 1 supports this view. The ratios, on the other hand, also include the (dominant) perturbative contribution. Thus, in order to calculate $\kappa_{(2)}$ including this contribution, we use the fact that $\int_0^1 x(\bar{d}(x) - \bar{u}(x))dx \neq 0$ from non-perturbative effects only, and rewrite (1) as

$$\kappa_{(2)} = 1 + \frac{\int_0^1 dx x [\bar{d}(x) - \bar{u}(x)]^{\text{NP}}}{\int_0^1 dx x \bar{u}(x)}, \quad (16)$$

where in the denominator we have used the CTEQ parameterization [6] for the integral of the \bar{u} antiquark distribution. The obtained value is

$$\kappa_{(2)} = 1.22, \quad (17)$$

compatible with the values quoted in the introduction.

For the Gottfried sum rule (12), we obtain $S_G = 0.255$, which is to be compared with the experimental value 0.235 ± 0.026 , obtained by the E866 collaboration [1, 2]. The calculation of the multiplicities through (10) give $n_{\pi N} \simeq 0.30$ and $n_{\pi \Delta} \simeq 0.27$.

Before moving to the strange sector, it is worth noticing that this value of $\kappa_{(2)}$ indicates a violation of $SU(2)$ flavor inside the proton which is not in conflict with the $SU(2)$ charge symmetry between the proton and the neutron. The $SU(2)$ charge symmetry still holds in the MCM. In order to check this, it is enough to write the dominant terms of the Fock expansion for the neutron cloud

$$|n\rangle = Z[|n_0\rangle + |n_0\pi^0\rangle + |p\pi^-\rangle + |\Delta^0\pi^0\rangle + |\Delta^+\pi^-\rangle + |\Delta^-\pi^+\rangle], \quad (18)$$

and realize that, since our coupling constants respect $SU(2)$, it follows that $g_{np\pi^-} = g_{pn\pi^+}$, $g_{n\Delta^-\pi^+} = -g_{p\Delta^+\pi^-}$, and $g_{n\Delta^+\pi^-} = -g_{p\Delta^0\pi^+}$. When we substitute these relations in (11) and use $m_p = m_n$, we arrive at the conclusion that $\bar{d}(x) - \bar{u}(x)$ in the proton is exactly the same as $\bar{u}(x) - \bar{d}(x)$ in the neutron.

In Figs. 3a-c we show, respectively, $xs(x)$ (compared to $x\bar{s}$), $x(s(x) - \bar{s}(x))$ (decomposed in its octet and decuplet contributions), and $s(x) - \bar{s}(x)$ as functions of x . Using $SU(3)$ symmetry for the baryons, we assume that the valence $s(x)$ distribution in the hyperons is the same as the valence $d(x)$ distribution in the proton [8]. This assumption is compatible with the others made previously concerning the $SU(3)$ symmetry at the hadronic level, namely, that the coupling constants follow $SU(3)$ and that the cut-off parameters are the same within the $SU(3)$ multiplets⁴. The $s(x)$ quark distribution is harder than the $\bar{s}(x)$ distribution because it is inside a (harder) strange

⁴ Even with these assumptions we will find below a $SU(3)$ breaking effect at the partonic level ($\kappa_{(3)} \neq 1$)

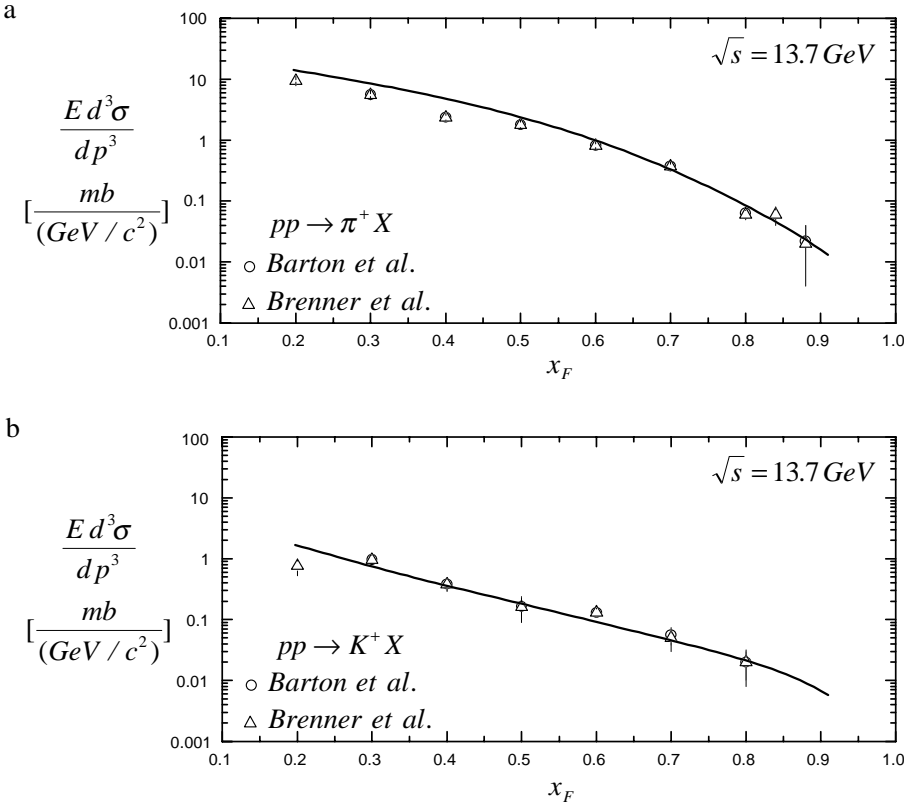


Fig. 2. **a** Inclusive pion spectrum measured in [25, 26] and computed with the meson cloud model of [16] and parameters given in (14); **b** the same as **a** for the kaon spectrum

baryon in the cloud, a conclusion corroborated by other authors [27]. In Fig. 3b we can appreciate how significant the decuplet contribution is for the $x(s(x) - \bar{s}(x))$ asymmetry, which is plotted in Fig. 3c against the experimental result (shaded area) [3].

In Fig. 4 we show $\bar{s}(x) - \bar{u}(x)$ in the proton. The points represent the parameterizations CTEQ4L (full circles), GRV98LO (open circles) and MRS99-1 (squares) and the solid line shows the MCM result. The dashed and dotted lines show the octet and decuplet contributions to the meson cloud, respectively. From this figure we can see that the decuplet contribution is sizable, and therefore it should be included in any study of non-singlet quantities involving the strange sea quark distributions.

When extending our analysis from 2 to 3 flavors, we can define a quantity analogous to the $\bar{d}(x) - \bar{u}(x)$ difference, i.e., a quantity which measures how blocked the production of strange quarks is, compared to the non-strange quarks: $\bar{d}(x) + \bar{u}(x) - s(x) - \bar{s}(x)$. Notice that, from the point of view of perturbative QCD, this quantity should be zero (besides, perhaps, some small mass effects, which should not be relevant in the intermediate or small x region). Hence, if our current view of the non-perturbative proton sea, as generated from mesons and from Pauli blocking, is correct this difference should also be well described by the MCM. We show our results in Fig. 5, and we see that our MCM curve (solid line) is compatible (although on the edge) with the values extracted from the different parameterizations for the parton distribution functions. We then conclude that the proportion of strange to non-strange quarks as calculated in the MCM is

compatible with what the standard parameterizations for parton distributions tell us. For illustration, we also show in the dashed lines what would be $\bar{d}(x) + \bar{u}(x) - s(x) - \bar{s}(x)$ in the $SU(3)$ symmetry limit, which will be defined in (23).

The combination of parton distributions shown in Fig. 5 is useful for the computation of the factor $\kappa_{(3)}$. Indeed, the numerator and denominator of (2) can be rewritten, as before, as sums of a perturbative (P) plus a non-perturbative (NP) contributions:

$$\int_0^1 dx x [s + \bar{s}](x) = \int_0^1 dx x [(s + \bar{s})^P + (s + \bar{s})^{NP}](x), \quad (19)$$

$$\int_0^1 dx x [\bar{u} + \bar{d}](x) = \int_0^1 dx x [(\bar{u} + \bar{d})^P + (\bar{u} + \bar{d})^{NP}](x). \quad (20)$$

Subtracting (20) from (19), dividing both sides by (20), and assuming that all the perturbative contributions cancel in the numerator, we rewrite $\kappa_{(3)}$ as

$$\kappa_{(3)} = 1 + \frac{\int_0^1 dx x [s + \bar{s}]^{NP}(x) - \int_0^1 dx x [\bar{u} + \bar{d}]^{NP}(x)}{\int_0^1 dx x [\bar{u} + \bar{d}](x)}, \quad (21)$$

where, as in (16), we have used the CTEQ4 [6] parameterizations in the denominator. In the above expressions the non-perturbative quantities are calculated with the MCM. Using the parameters described before we find

$$\kappa_{(3)} = 0.55, \quad (22)$$

in reasonable agreement with the value quoted by the CCFR collaboration [3]. We have checked that this number might change by $\sim 10\%$ if other parameterizations

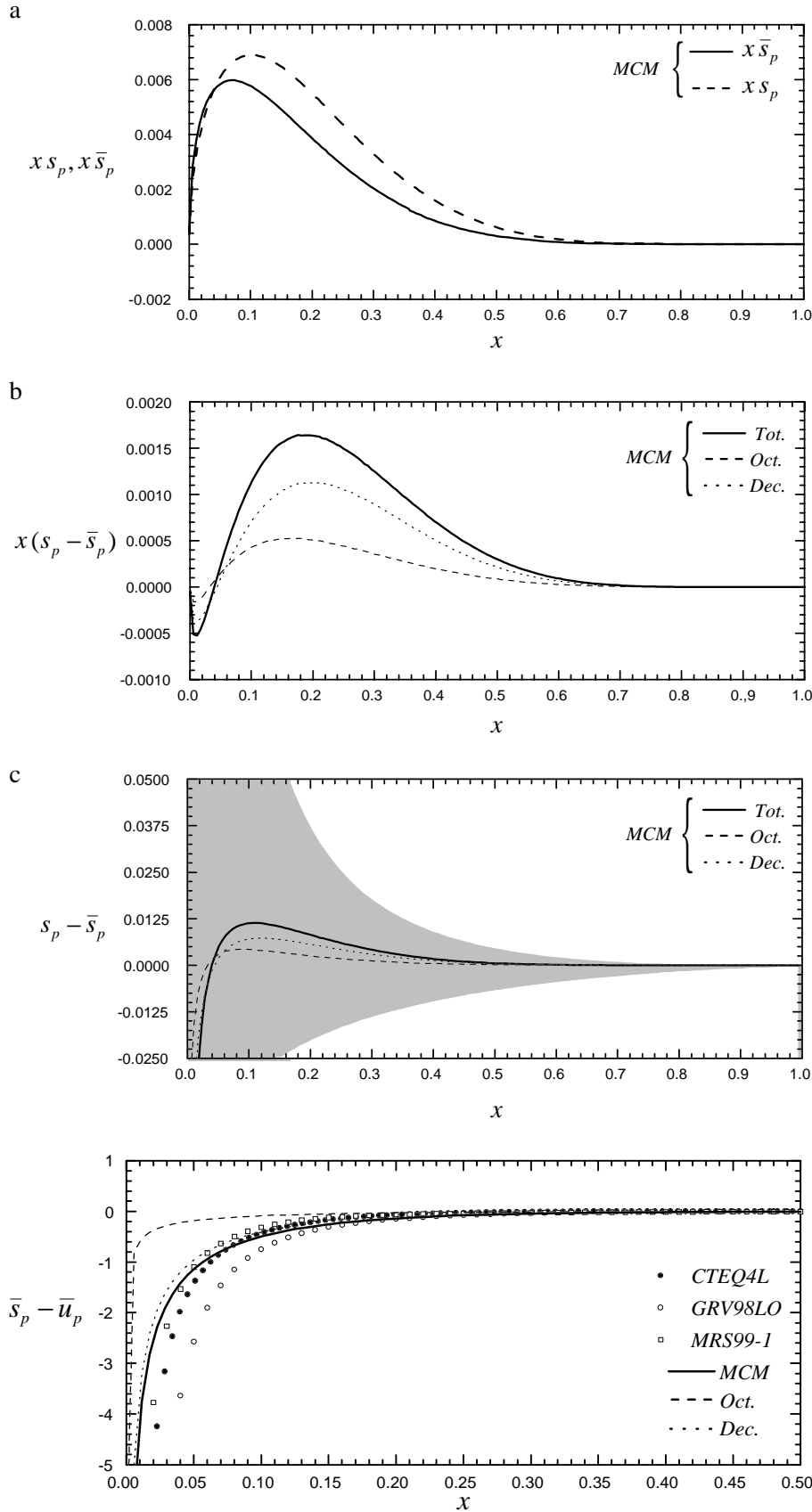


Fig. 3. **a** $x\bar{s}(x)$ (solid line) and $xs(x)$ (dashed line) in the proton computed with the MCM (using (11)); **b** $x(s(x) - \bar{s}(x))$ in the proton in the MCM. The octet and decuplet contributions are represented by the dashed and the dotted lines, respectively; **c** same as **b** for the difference $s(x) - \bar{s}(x)$. The shaded area is the uncertainty range of the experimental data [3]

Fig. 4. $\bar{s}(x) - \bar{u}(x)$ in the proton extracted from several parameterizations, and the resulting curves from the MCM (solid line). The octet and decuplet contributions are the dashed and the dotted lines, respectively

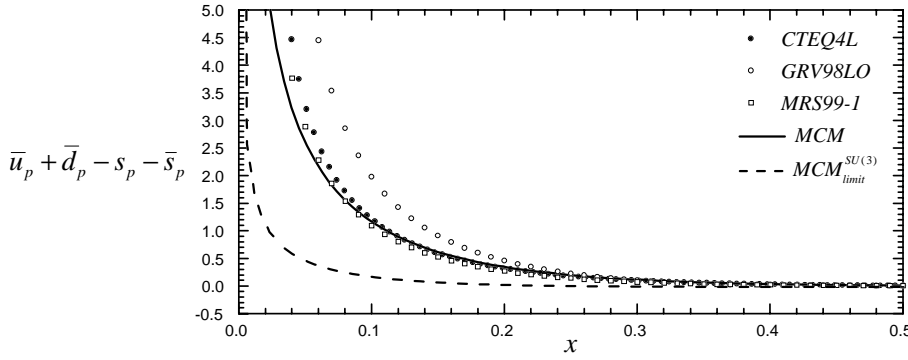


Fig. 5. $\bar{u}(x) + \bar{d}(x) - s(x) - \bar{s}(x)$ in the proton extracted from several parameterizations, and the result from the MCM (solid line). The dashed line is the MCM in the $SU(3)$ limit

(GRV98, MRS99) were used. This would not qualitatively change our conclusions. Therefore, we use only the CTEQ parameterization in our analysis.

The cloud parameters used so far give an overall good agreement with the available experimental information. However, they are not the result of a best fit, and a different set of parameters could yield good results as well. In particular, we would like to mention that our value for $g_{p\Delta^0\pi^+}$ is somewhat large (although still compatible with the data) and, as was argued in [15], a value about 30% smaller might be more appropriate. We repeated our calculation using $g_{p\Delta^0\pi^+} = 22.0/6^{1/2}$. The cut-off parameters had to be changed to $\Lambda_{\text{oct}} = 1.11$ GeV and $\Lambda_{\text{dec}} = 1.15$ GeV, and the new multiplicities were calculated to be $n_{\pi N} \simeq 0.30$ and $n_{\pi\Delta} \simeq 0.19$. On the other hand, $\kappa_{(3)} = 0.66$ with this new set of parameters, implying less agreement between the model and the experimental data.

We now take the $SU(3)$ symmetry limit, which means in our case to make the masses equal within the multiplets⁵, i.e.,

$$\begin{aligned} m_{\text{meson}}^{\text{octet}} &= (m_{\pi} + m_K)/2, \\ m_{\text{baryon}}^{\text{octet}} &= (m_p + m_n + m_{\Sigma} + m_{\Lambda})/4, \\ m_{\text{baryon}}^{\text{decuplet}} &= (m_{\Sigma^*} + m_{\Delta})/2. \end{aligned} \quad (23)$$

As $\kappa_{(3)}$ in (21) measures the amount of symmetry breaking between the strange and non-strange quarks, it is remarkable that within our $SU(3)$ symmetry limit, we have $\kappa_{(3)} = 0.96$, which is in good agreement with $\kappa_{(3)} = 1$. We see, therefore, that in making the cloud $SU(3)$ symmetric, we recover the $SU(3)$ flavor symmetry in the parton distributions.

It is of capital importance to compare the $SU(3)$ symmetry limit, as defined by (23), with a similar limit in the $SU(2)$ case. Notice that to calculate the $\bar{d}(x) - \bar{u}(x)$ difference, we are already using a limit similar to that of (23). That is, we have only one mass in the meson octet, m_{π} , only one mass in the baryon octet, $m_p = m_n$, and only one mass in the baryon decuplet, as only the Δ is relevant in that case. The bulk of the $\bar{d}(x) - \bar{u}(x)$ difference comes, then, from the mass difference *between* the octet

⁵ Other choices for the values of the masses in the symmetry limit would, of course, result in a different value for $\kappa_{(3)}$, for instance. The important point is that equal masses within the multiplets indicate a tendency to recover the $SU(3)$ symmetry

Table 3. Σ^+ octet coupling constants

$g_{\pi^+\Lambda\Sigma^+}$	$(2/3^{1/2})2\alpha_D g_{p\pi^0 p}$
$g_{K^+\Sigma^+\Xi^0}$	$-g_{p\pi^0 p}$
$g_{\Sigma^+\Sigma^+\pi^0}$	$2(1 - \alpha_D)g_{p\pi^0 p}$
$g_{p\bar{K}^0\Sigma^+}$	$2^{1/2}(2\alpha_D - 1)g_{p\pi^0 p}$
$g_{\Sigma^+\pi^+\Sigma^0}$	$2(1 - \alpha_D)g_{p\pi^0 p}$

and decuplet baryon masses. We have checked that when $m_p \sim m_{\Delta}$, $\kappa_{(2)} \sim 1$. For the $\bar{d}(x) + \bar{u}(x) - s(x) - \bar{s}(x)$ difference, however, the important contribution comes from the mass differences *inside* the octet and decuplet states.

2.2 The sigma

For the Σ^+ baryon we consider the following expansion:

$$\begin{aligned} |\Sigma^+\rangle &= Z[|\Sigma_0^+\rangle + |\Sigma^+\pi^0\rangle + |\Sigma^0\pi^+\rangle + |\Lambda^0\pi^+\rangle \\ &+ |p\bar{K}^0\rangle + |\Xi^0 K^+\rangle + |\Delta^{++}K^-\rangle + |\Delta^+\bar{K}^0\rangle \\ &+ |\Sigma^{*+}\pi^0\rangle + |\Sigma^{*0}\pi^+\rangle + |\Xi^{*0}K^+\rangle]. \end{aligned} \quad (24)$$

We included the $|\Xi^0 K^+\rangle$ and the decuplet states in the second line of (24). These states were not considered in [7], and the authors of [9] considered only the two lowest lying decuplet states ($|\Sigma^{*+}\pi^0\rangle, |\Sigma^{*0}\pi^+\rangle$). It will be seen here that the decuplet states play an important role in the x dependence of the parton distributions, in spite of their large masses.

The parton distributions in the Σ^+ sea can be straightforwardly computed through (5)–(11), where the relevant replacements of masses and couplings have to be made. Following the steps of Sect. 2.1, we take the couplings according to the $SU(3)$ relations [17]. Hence, for the octet coupling constants we see the entries of Table 3.

For the decuplet couplings we have Table 4. For the cut-off parameters, we will use the same values as given by (14).

In Fig. 6 we show the separate contributions from the octet and decuplet states for $x(\bar{d}(x) - \bar{u}(x))$ (a), $x(\bar{d}(x) - \bar{s}(x))$ (b), $x(\bar{u}(x) - \bar{s}(x))$ (c). The total distributions are shown in the Fig. 6d, and they should be compared with Fig. 4 of [7]. We qualitatively agree with them. Quantitative changes are noticeable, and they occur because of the

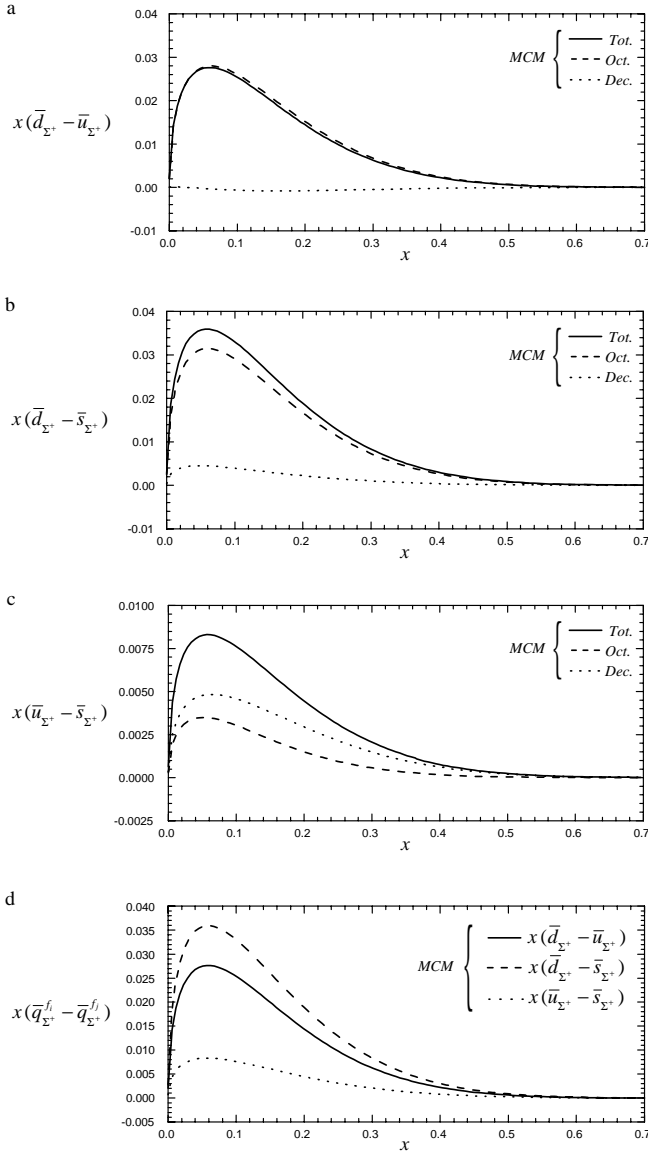


Fig. 6. **a** $x(\bar{d}(x) - \bar{u}(x))$ in the Σ^+ calculated with the MCM (solid line). The octet and decuplet contributions are the dashed and dotted lines, respectively; **b** same as **a** for $x(\bar{d}(x) - \bar{s}(x))$; **c** same as **a** $x(\bar{u}(x) - \bar{s}(x))$; **d** all the curves together, where the decuplet and octet contributions were added

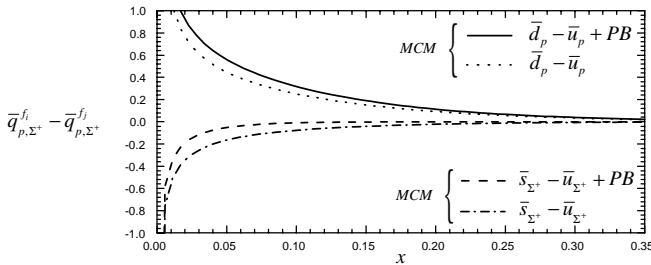


Fig. 7. $x(\bar{d}(x) - \bar{u}(x))$ in the proton, with (solid line) and without (dotted line) Pauli blocking. $(\bar{s}(x) - \bar{u}(x))$ in the Σ^+ , with (dashed line) and without (dot-dashed line) Pauli blocking. All the curves were calculated in the MCM

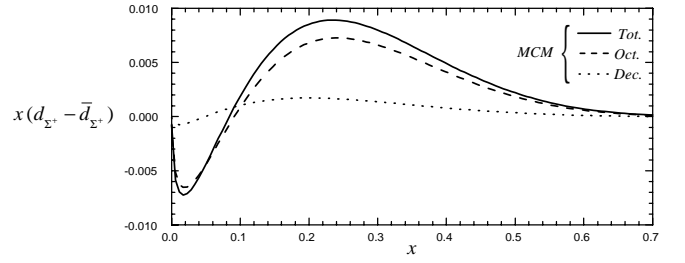


Fig. 8. $x(d(x) - \bar{d}(x))$ in the Σ^+ with the MCM. The octet and decuplet contributions are the dashed and the dotted lines, respectively

Table 4. Σ^+ decuplet coupling constants

$g_{\Sigma^+ \Delta^+ \bar{K}^0}$	$g_{p \Delta^0 \pi^+}$
$g_{\Sigma^+ \Delta^+ K^-}$	$3^{1/2} g_{p \Delta^0 \pi^+}$
$g_{\Sigma^+ \Xi^0 K^+}$	$g_{p \Delta^0 \pi^+}$
$g_{\Sigma^+ \Sigma^0 \pi^+}$	$-(1/2^{1/2}) g_{p \Delta^0 \pi^+}$
$g_{\Sigma^+ \Sigma^+ \pi^0}$	$-(1/2^{1/2}) g_{p \Delta^0 \pi^+}$

inclusion of the decuplet states which play a significant role, as seen in Figs. 6b,c. The fact that $x(\bar{d}(x) - \bar{u}(x)) > x(\bar{u}(x) - \bar{s}(x))$ was interpreted in [7,9] as a violation of $SU(3)$ charge symmetry, and this really seems to be the case. Even more indicative of this breaking is the direct comparison of $x(\bar{d}(x) - \bar{u}(x))$ in the proton (dotted line) with $x(\bar{s}(x) - \bar{u}(x))$ in the Σ^+ (dot-dashed line), shown in Fig. 7. A huge discrepancy is seen between the two curves, a result in complete disagreement with naive expectations. As in the quark model the Σ^+ is a proton with the d quark replaced by an s quark, naively one would think that $x(\bar{d}(x) - \bar{u}(x))$ in the proton is equal to $x(\bar{s}(x) - \bar{u}(x))$ in the Σ^+ .

As we saw in Sect. 2, the PB effect is important in describing the x dependence of the light quark sea asymmetry. From the point of view of Fermi statistics, the same effect should be present in the Σ^+ , with the s quark here playing the role of the d quark in the proton. Because of the mass of the s quark, the x dependence of the PB in the Σ^+ may not be exactly the same as in the proton. However, to exemplify the size of the corrections from PB, we also plot in Fig. 7 the distributions including the effect of the PB given by (13). The solid line is for $x(\bar{d}(x) - \bar{u}(x))$ in the proton, and the dashed line is for $x(\bar{s}(x) - \bar{u}(x))$ in the Σ^+ .

It seems also appropriate to extend the comparisons to $d(x) - \bar{d}(x)$ in the Σ^+ , and to $s(x) - \bar{s}(x)$ in the proton. We show the $d(x) - \bar{d}(x)$ in Fig. 8, where the decuplet and octet contributions are shown separately. In Fig. 9 we show both differences and we clearly see the discrepancy between them, which is again evidence of $SU(3)$ charge symmetry breaking. It is remarkable, however, that besides the small mass of the d quark, the $d(x) - \bar{d}(x)$ asymmetry in the Σ^+ is much larger than the $s(x) - \bar{s}(x)$ asymmetry in the proton.

Finally, in order to compare the $SU(3)$ flavor breaking in sea parton distributions in the Σ^+ with the pro-

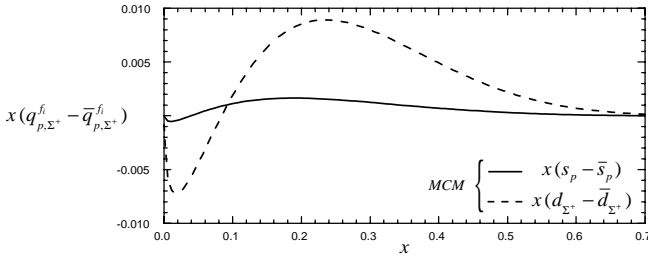


Fig. 9. $x(s(x) - \bar{s}(x))$ in the proton (solid line) and $x(d(x) - \bar{d}(x))$ in the Σ^+ (dashed line). Both curves were calculated in the MCM

ton, we compute $\kappa_{(3)}$ defined in (21). The denominator in (21) is governed by the large perturbative contributions and is only slightly affected by the cloud component. It is therefore reasonable to assume that it is the same for the proton and for the Σ^+ . In the numerator we have approximated $\int dx x [s + \bar{s}]^{\text{NP}}$ by $\int dx x [2\bar{s}]^{\text{NP}}$ in order to avoid uncertainties associated with $s(x)$ in the hyperon. The resulting value for κ_3 is then

$$\kappa_3 \simeq 0.85. \quad (25)$$

This value of κ_3 indicates a violation of $SU(3)$ flavor inside the Σ^+ which is weaker than that inside the proton, whereas Figs. 5–8 show a violation of the $SU(3)$ symmetry between the proton and the sigma. Both symmetries are restored in the $SU(3)$ symmetry limit of (23), i.e., $\kappa_3 \rightarrow 1$ and the curves in the figures assume their expected behavior, with $d_{\Sigma^+} = s_p$ and $\bar{d}_{\Sigma^+} = \bar{s}_p$.

In the context of the meson cloud model this result is not surprising. The cloud expansion of the Σ^+ involves heavier states than those appearing in the proton expansion. As a consequence, the whole Σ^+ cloud will be suppressed with respect to the proton cloud. Indeed, looking at the multiplicities we observe that the probabilities associated with the hyperon states are typically one order of magnitude smaller than those associated with the proton states. Moreover, the strange states inside the proton are heavier and suppressed with respect to non-strange states, and therefore we expect (and actually observe) $\bar{d} > \bar{u} > \bar{s}$. Neglecting Pauli-blocking effects (which would slightly inhibit the \bar{s} production in comparison with the \bar{d} production in the Σ^+), we would expect the same behavior for the Σ^+ and this is exactly what we find. Quantitatively, the suppression of \bar{s} in Σ^+ (with respect to \bar{d} or \bar{u}) happens because all the states in the cloud contain strangeness and are nearly equally suppressed. In the proton the suppression of \bar{s} (always with respect to \bar{d} or \bar{u}) is more pronounced because of the mass difference between strange and non-strange cloud states.

3 Conclusions

In this work we have applied the meson cloud model to study the non-perturbative aspects of parton distributions, giving special emphasis to the strange sector. We have adjusted the cloud cut-off parameters to reproduce the

E866 data on $\bar{d}(x) - \bar{u}(x)$ and $\bar{d}(x)/\bar{u}(x)$. In this procedure the choices were not completely free. Instead, the cut-off values had to be consistent with previous analyses of other experimental information [16]. Having fixed the parameters we moved to the strange sector. In this sense, the results for the strange–anti-strange asymmetry and for $\bar{u} + \bar{d} - s - \bar{s}$ can be considered as predictions. They are consistent with the data. Finally, we have taken the $SU(3)$ limit in the meson cloud and found that, in this limit, the parton distributions become $SU(3)$ flavor symmetric, i.e., $\kappa \rightarrow 1$. We have thus presented additional experimental confirmation of the MCM. Moreover we have concluded that the meson cloud is responsible for the $SU(3)$ flavor breaking in parton distributions.

Acknowledgements. This work has been supported by CNPq and FAPESP under contract number 98/2249-4. We are indebted to C. Schat, W. Melnitchouk and A. W. Thomas for discussions.

A Appendix

For the sake of completeness we list in this appendix the parton distributions used in our calculations.

The LO parton distributions in the pion are given by the GRS98 parameterization [4]:

$$xq_v^\pi(x, Q^2) = Nx^a(1 + A\sqrt{x} + Bx)(1-x)^D, \quad (\text{A.1})$$

and we neglect the sea content in the meson, that is,

$$\begin{aligned} \bar{d}^{\pi^+} &= u^{\pi^+} = \bar{u}^{\pi^-} = d^{\pi^-} = \frac{1}{2}q_v^\pi, \\ \bar{u}^{\pi^0} &= u^{\pi^0} = \bar{d}^{\pi^0} = d^{\pi^0} = \frac{1}{4}q_v^\pi, \end{aligned} \quad (\text{A.2})$$

with

$$\begin{aligned} N &= 1.212 + 0.498s + 0.009s^2, \quad a = 0.517 - 0.020s, \\ A &= -0.037 - 0.578s, \end{aligned}$$

$$B = 0.241 + 0.251s, \quad D = 0.383 + 0.624s, \quad (\text{A.3})$$

where

$$s \equiv \ln \frac{\ln[Q^2/\Lambda^2]}{\ln[\mu_{LO}^2/\Lambda^2]}, \quad (\text{A.4})$$

is evaluated for $\mu_{LO}^2 = 0.26 \text{ GeV}^2$ and $\Lambda^2 = (0.204 \text{ GeV})^2$, valid for $0.31 \lesssim s \lesssim 2.2$ (i.e. $0.5 \lesssim Q^2 \lesssim 10^5 \text{ GeV}^2$) and $10^{-5} \lesssim x < 1$.

For the LO parton distributions in the kaon, we also employ the GRS98 parameterization [4]:

$$\begin{aligned} \bar{u}^{K^-} &= u^{K^+} = d^{K^0} = \bar{d}^{\bar{K}^0} = 0.541(1-x)^{0.17}q_v^\pi, \\ \bar{s}^{K^+} &= \bar{s}^{K^0} = s^{\bar{K}^0} = s^{K^-} = q_v^\pi - u^{K^+}. \end{aligned} \quad (\text{A.5})$$

The LO parton distributions in the proton are given by the CTEQ4L parameterization [6] at $Q_0 = 1.6 \text{ GeV}$:

$$xq^p(x, Q_0^2) = A_0 x^{A_1} (1-x)^{A_2} (1 + A_3 x^{A_4})$$

Parton	A_0	A_1	A_2	A_3	A_4
xu_v^p	1.226	0.443	3.465	7.589	1.146
xd_v^p	0.702	0.443	4.003	2.433	0.622
$xs(\bar{s})^p$	0.050	-0.200	6.877	5.644	1.000

(A.6)

References

1. E.A. Hawker et al., E866/NuSea Collab., Phys. Rev. Lett. **80**, 3715 (1998)
2. J.C. Peng et al., E866/NuSea Collab., Phys. Rev. D **58**, 092004 (1999)
3. A.O. Bazarko et al., CCFR Collab., Z. Phys. C **65**, 189 (1995)
4. M. Glück, E. Reya, M. Stratmann, Eur. Phys. J. C **2**, 159 (1998); M. Glück, E. Reya, A. Vogt, Eur. Phys. J. C **5**, 461 (1998); M. Glück, E. Reya, I. Schleinbein, Eur. Phys. J. C **10**, 313 (1999)
5. A.D. Martin, W.J. Stirling, R.G. Roberts, R.S. Thorne, Phys. Rev. D **51**, 4756 (1995)
6. H.L. Lai et al., CTEQ, Phys. Rev. D **55**, 1280 (1997)
7. F. Cao, A.I. Signal, Phys. Lett. B **474**, 138 (2000)
8. M. Alberg, T. Falter, E.M. Henley, Nucl. Phys. A **644**, 93 (1998); M. Alberg, E.M. Henley, X. Ji, A.W. Thomas, Phys. Lett. B **389**, 367 (1996)
9. C. Boros, A.W. Thomas, Phys. Rev. D **60**, 074017 (1999)
10. P.G. Ratcliffe, Phys. Lett. B **365**, 383 (1996)
11. H. Kim, T. Doi, M. Oka, S.H. Lee, Nucl. Phys. A **662**, 371 (2000)
12. M.E. Bracco, F.S. Navarra, M. Nielsen, Phys. Lett. B **454**, 346 (1999)
13. A.W. Thomas, Phys. Lett. B **126**, 97 (1983)
14. For a recent review see J. Speth, A.W. Thomas, Adv. Nucl. Phys. **24**, 83 (1998); S. Kumano, Phys. Rep. **303**, 183 (1998)
15. W. Melnitchouk, J. Speth, A.W. Thomas, Phys. Rev. D **59**, 014033 (1999)
16. F. Carvalho, F.O. Durães, F.S. Navarra, M. Nielsen, Phys. Rev. D **60**, 094015 (1999)
17. J.J. de Swart, Rev. Mod. Phys. **35**, 916 (1963); **37**, 1326(E) (1965)
18. M. Przybycien, A. Szczurek, G. Ingelman, Z. Phys. C **74**, 509 (1997)
19. R.G.E. Timmermans, Th.A. Rijken, J.J. de Swart, Phys. Lett. B **257**, 227 (1991)
20. W. Koepf, L.L. Frankfurt, M. Strikman, Phys. Rev. D **53**, 2586 (1996)
21. R.M. Davidson, N.C. Mukhopadhyay, Phys. Rev. D **42**, 20 (1990); R.M. Davidson, N.C. Mukhopadhyay, R. Wittman, Phys. Rev. D **43**, 71 (1991)
22. R.D. Field, R.P. Feynman, Phys. Rev. D **15**, 2590 (1977)
23. J.F. Donoghue, E. Golowich, Phys. Rev. D **15**, 3421 (1977)
24. F.M. Steffens, A.W. Thomas, Phys. Rev. C **55**, 900 (1997)
25. D.S. Barton et al., Phys. Rev. D **27**, 2580 (1983)
26. A.E. Brenner et al., Phys. Rev. D **26**, 1497 (1982)
27. S.J. Brodsky, Bo-Quiang Ma, Phys. Lett. B **381**, 317 (1996)
28. W. Melnitchouk, M. Malheiro, Phys. Lett. B **451**, 224 (1999)